

# Galactic cosmic rays above the Earth's atmosphere

**Marusya Buchvarova**

Space Research and Technology Institute-BAS  
Acad. Georgi Bonchev Str., bl. 1, Sofia 1113, Bulgaria

Corresponding author: [marusjab@yahoo.com](mailto:marusjab@yahoo.com)

**Abstract.** Galactic cosmic rays (GCRs) originate from sources outside the solar system and reach the Earth's environment from all directions. More than 100 years after the first detection of cosmic rays, the origin of high-energy cosmic rays is still a mystery. Although our knowledge of the origin and propagation of cosmic rays is relatively limited, we can study the radiation conditions in the near-Earth space environment in more detail. The origin, composition, and energy spectra of cosmic rays are briefly discussed in this paper. A brief review of the transport of galactic cosmic rays in the heliosphere is given. The geomagnetic effects on galactic cosmic rays and the atmospheric interactions of primary particles are also discussed in the paper.

## 1. Introduction

The discovery of cosmic rays by Victor Hess in 1912 opened a new window for the matter in the Universe. The beginning of a whole new world of particles beyond the confines of the atom was set [1]. The first particle of antimatter, the positron, was discovered in 1932, the muon was discovered in 1936, followed by the pion, the kaon, and many others. In 1956, the Cowan–Reines neutrino experiment confirmed the existence of neutrinos; until then, the neutrino had been a purely hypothetical particle. Today, we know that galactic cosmic rays travel through interstellar space and the heliospheric magnetic field, leading to a strong modulation of their spectrum, and also pass through the Earth's magnetosphere before reaching us.

In the near-Earth space, the main sources of corpuscular radiation are galactic cosmic rays (GCRs), particles of solar origin as solar energetic particles (SEPs), and particles trapped in the Earth's magnetosphere (radiation belts). Before cosmic rays (CRs) interact in the atmosphere they are known as primary cosmic rays (PCRs). Although cosmic rays include galactic cosmic rays and other classes of energetic particles, including solar energetic particles and particles accelerated in interplanetary space, the term “cosmic rays” is often used to refer only to galactic cosmic rays.

Galactic cosmic rays are charged particles originating in sources outside the Solar system that travel through space at nearly the speed of light, and reach the Earth from all directions. They consist of ionized nuclei, mainly protons, some helium, and less than 1% heavier elements. Among the cosmic rays, other subatomic particles (besides protons) can also be found. The particles with intrinsic mass are known as “cosmic rays” while photons, which are quanta of electromagnetic radiation (and therefore have no intrinsic mass), are called by their common names such as gamma rays or X-rays, depending on their photon energy [2].

Cosmic rays can have a wide range of energies, from tens of MeV to  $10^{20}$  eV. Particles with energies less than 30 MeV/nuc are often neglected in descriptions of space radiation environments because their range is so small that they would not pass through typical shielding levels [3]. The low-energy cosmic



rays can only be detected at high latitudes and altitudes. Their spectra can be recorded onboard spacecraft, rockets, and balloons [4]. In the energy range above 1 GeV, CR spectra are well measured by ground-based neutron monitors and muon telescopes.

Cosmic ray particles are divided into two main classes depending on their energy and probable acceleration sites [5]: charged particles with energies less than  $10^{18}$  eV are referred to as galactic cosmic rays; above that energy ( $\sim 10^{18}$  eV), they are referred to as extragalactic cosmic rays or ultrahigh-energy cosmic rays. Although galactic cosmic rays are thought to be accelerated in the shock waves generated by powerful supernova explosions [5], the sources and sites of cosmic ray acceleration are still debatable. In addition, the origin of the highest-energy particles remains a mystery. By comparison, the most powerful man-made particle accelerator, the Large Hadron Collider near Geneva, reaches energies of  $10^{13}$  eV, which is barely one ten-millionth of the energy of the registered cosmic rays with the highest energy [5].

The magnetic fields of our Galaxy have two different components: a regular and a turbulent one [6]. The strength and directions of the magnetic fields that belong to the turbulent component are random [6, 7, 8]. The charged particles are deflected by the magnetic fields in the galaxy, so there is virtually no connection between the directions from which the particles seem to come to us and the directions of their sources. The cosmic ray flux that arrives at the Earth is also random or, more precisely, isotropic [6]. For this reason, it is difficult to identify specific astronomical objects as sources of cosmic rays. The particle flux is not only isotropic but also approximately constant in time, so the GCRs create a nearly uniform background of ionizing radiation that hits the Earth's atmosphere. Due to extremely high energies, high-energy cosmic radiation is the most penetrating type of cosmic radiation in the Earth's atmosphere.

## 2. Origin and composition of galactic cosmic rays

Cosmic rays come from all over the Universe. Particles with energies up to  $\sim 10^{18}$  eV must be accelerated by galactic sources. Above that energy, their sources must have extragalactic origin, although the exact demarcation energy remains somewhat vague and debatable, and there could be some overlap [5]. Galactic nuclei are believed to be accelerated at supernova remnant (SNR) shocks via first-order Fermi mechanism and to be then somehow released into the ISM, where they reside for some time before escaping the Galaxy [9]. This is the so-called SNR paradigm for the origin of galactic cosmic rays [10]. However, some types of expanding supernova remnants, for example, are estimated not to be able to accelerate protons above energies in the range of  $10^{15}$  eV [11]. Possible sources of protons with those energies are massive star clusters (can reach PeV energies) [12] as well as the Galactic Center region [13]. The question remains whether the acceleration mechanism working in the SNRs can increase the energy of the particles all the way to the PeV region and beyond. What is the capability of SNRs to accelerate galactic cosmic rays to these extreme energies is an open question that requires more in-depth research. Cosmic rays with energies above  $\sim 10^{18}$  eV are thought to be of extragalactic origin. Their sources are not known. Candidates for sources range from the birth of compact objects to explosions related to gamma-ray bursts or to events in active galaxies [14, 15].

According to Ginzburg & Syrovatskii (1964) [16]: "Any theory of the origin of cosmic rays cannot expect serious success unless it rests on a detailed analysis of the observed composition of primary cosmic radiation". All-natural elements from the periodic table are present in the composition of cosmic rays. The main features of the cosmic ray composition at low energies ( $< 10^{14}$  eV) are well-known, but at higher energies, they remain unclear [17]. It is generally believed that the cosmic ray "knee" at  $10^{15}$  eV may reflect a gradual transition towards a heavier composition [18]. In the direct-measurement energy region, about 98% of the particles are protons and nuclei;  $\approx 2\%$  are electrons [19]. Of the protons and nuclei,  $\approx 87\%$  are protons (H),  $\approx 12\%$  are helium nuclei (He) and a small fraction of  $\approx 1\%$  are heavier nuclei [19]. GCR nuclei of elements whose charge  $Z$  is higher than that of helium (with a charge of +2) are called HZE ions. De Angelis and Pimenta note in [20] that the composition is expected to vary with energy; however, only the energies below the knee are responsible for the known proportions. Cosmic rays in the Galaxy consist of two components: a primary component, representing the composition of

the source, and a secondary component (Li, Be, B, sub-iron elements) produced by the interactions of the primaries with interstellar gas. Note that “primary” and “secondary” are used in a different but analogous sense when discussing cosmic ray interactions in the atmosphere [11].

### 3. Cosmic ray energy spectrum

The primary cosmic-ray particles extend over at least 13 decades in energy, with a corresponding decline in intensity of over 32 decades [21]. The all-particle CR spectrum obtained by compiling data from various instruments is shown in figure 1.

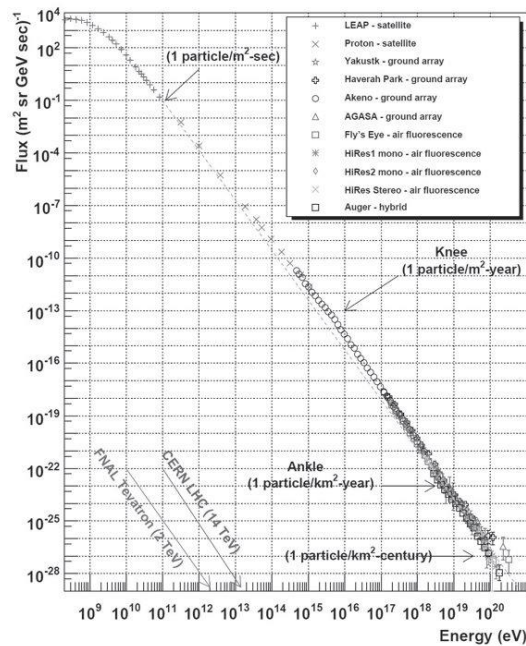


Figure 1. The overall differential energy spectra of cosmic rays from various experiments. Important features in the CR spectrum are indicated: the “knee” at  $10^{15}$  eV and the “ankle” at  $10^{18}$  eV. The frequencies of arrival of particles of different energies are pointed out, as well as the energies achievable in various accelerator experiments (Image from [22]).

The differential energy spectrum  $D(E)$  is defined as the number of particles  $dN$  observed by a detector in the energy band from  $E$  to  $E + dE$  passing through a unit surface area  $dA$  and arriving from a direction  $\Omega$  within a solid angle  $d\Omega$  during a time interval  $dt$  [6, 23]:

$$D(E) = \frac{dN}{dA \cdot dt \cdot d\Omega \cdot dE} \quad (3.1)$$

Here,  $D(E)$  is expressed in units of  $\text{m}^{-2} \text{s}^{-1} \text{sr}^{-1} (\text{MeV}/\text{nuc})^{-1}$ . As can be seen from figure 1, the GCR flux is a strongly decreasing function of energy. At first sight, the flux above a few GeV, where solar effects are negligible, can be approximated by a power law with a negative spectral index

$$D(E) \sim E^{-\gamma}, \quad (3.2)$$

$\gamma$  is the spectral index of the cosmic ray flux. This part of the CR flux represents the spectrum beyond the heliosphere and is called the Local Interstellar Spectrum (LIS) [23]. The spectrum is almost smooth, with some slight deviations from a constant power law.

Below  $E \sim 10^{15}$  eV, the power spectrum is a smooth curve with a spectral index of about 2.7. The energy spectra as a function of kinetic energy per nucleon of the primary ion components are very similar [24]. Below the knee, the statistics are still abundant enough and satellite and balloon experiments can provide information about the elemental composition of cosmic rays. In the conventional model for CR production, it is believed that the cosmic rays with the discussed energies are accelerated by astrophysical sources in our Galaxy, such as supernova remnants.

Two interesting features in the cosmic ray spectrum are observed: the “knee” and the “ankle”. Around the energy  $10^{15}$  eV the spectrum becomes steeper, defining the “knee”, and becomes flatter again above  $10^{18}$  eV. The knee of the spectrum is visible as a change in spectral index from 2.7 to 3. The origin of this feature is still under study. It is generally believed that at energies above  $\sim 10^{17-19}$  eV, the extragalactic CR particles dominate over the galactic ones. This seems to justify the hardening of the CR spectrum that defines another change in the slope, the so-called “ankle” [25, 26]. Here, the spectrum becomes less steep, and the spectral index changes back to  $\gamma \approx 2.7$ . It is believed that the threshold for the dominance of extragalactic sources is indeed close to the ankle [20]. In the energy interval between the knee and the ankle, the flux decreases significantly: there are only a few particles per square meter per year. Finally, at the highest energies, there is a drastic suppression of cosmic ray flux.

Cosmic rays with energies above  $10^{18}$  eV are known as ultrahigh-energy cosmic rays (UHECRs). The flux of the primaries at these energies is extremely low, of the order of 1 particle per  $\text{km}^2$  per century [27]. At the highest energies, cosmic rays are discovered by detectors with very large acceptance located on the surface of the Earth. The arrival rate of the most energetic particles is very low indeed, but particles with energies up to about  $10^{20}$  eV have been detected [22]. At these energies, a cut-off in the spectrum is expected due to the interaction with the cosmic microwave background (known as Greisen - Zatsepin – Kuzmin (GZK) effect). The limit, called the GZK-limit, was computed in 1966 by Kenneth Greisen, Vadim Kuzmin, and Georgiy Zatsepin. They predicted that cosmic ray protons with energies above the threshold energy of  $5 \cdot 10^{19}$  eV would interact with cosmic microwave background photons to produce pions [21]. This would continue until their energy falls below the pion production threshold [21]. However, the cosmological sources and acceleration mechanisms for UHECR particles are still unclear.

Galactic cosmic rays after accelerated at their sources, suffer a combination of processes including diffusion, reacceleration, convection, nuclear interactions, radioactive decay, and energy losses. The most widely used models describing the propagation of cosmic rays in the interstellar medium are the diffusion, Leaky Box, and weighted slab models. These models aim to explain the cosmic ray propagation in the interstellar medium. Upon arrival in the solar system, the behavior of galactic cosmic rays, especially at lower energies, is affected by the solar wind and its embedded heliospheric magnetic field (HMF). For particles with higher energies, the heliosphere becomes transparent.

The charged particles with energies below 30 GeV will experience solar modulation (see Section 4). Figure 1 shows that the modulated spectrum peaks at energies of several hundred MeV/nuc [23]. The flux at these energies is high. For example, the rate of arriving particles at energies of about  $10^9$  eV is  $\sim 10^4$  per square meter per second [21, 28]. Due to the interaction of galactic cosmic rays with the solar wind, our knowledge of the interstellar cosmic ray spectra at energies below a few GeV is obscured. Furthermore, because cosmic rays lose at least several hundred MeV/nuc when they traverse the inner heliosphere [29], we have essentially no information on the interstellar spectra of cosmic rays below  $\sim 200$  to  $\sim 300$  MeV/nuc [30]. Because of solar modulation and the fact that the nature of heliospheric diffusion coefficients is not yet fully established, all derived cosmic ray LIS at kinetic energies  $T \lesssim 1$  GeV remain contentious [31].

#### 4. Galactic cosmic rays in the heliosphere

Galactic cosmic rays (CRs) within the heliosphere interact with the solar wind and the heliospheric magnetic field embedded in it. This leads to significant global and temporal variations in their intensity and energy as a function of position inside the heliosphere [31]. The process is described as solar modulation [31]. The GCR modulation effect is strongest at the lowest observed energies and decreases

with increasing energy, until it vanishes (within the uncertainties) at around 30 GeV [32]. For higher energy particles, the heliosphere is transparent. The GCR modulated flux is anti-correlated with solar activity, i.e. low cosmic ray intensities are observed during solar maximum periods and vice versa during periods of solar minimum.

The dominant and most important periodicity in the variation of CR intensity associated with solar activity is the 11-year cycle. This quasi-periodicity is convincingly reflected in the sunspot record since the early 1600s and also in the galactic CR intensity observed since the 1950s by a global network of ground-based neutron monitors [31]. Note that other solar activity indicators also vary with the 11-year periodicity, such as solar wind parameters, heliospheric magnetic field, flares and coronal mass ejections, and others. The 11-year periodicity in solar activity is referred to as the solar cycle. However, the 11-year sunspot cycle is half of a longer, 22-year cycle of solar activity. The Sun reverses magnetic polarity (the north magnetic pole becomes the south and vice versa) around the maximum of each 11-year solar cycle. Thus, the complete magnetic cycle is, on average, about 22 years - twice the duration of the sunspot cycle [33]. Besides these cycles, some scientists believe that there are other, longer-period variations in the sunspot numbers and solar cycles [33]. However, most scientists think we need more data, spanning longer periods of time, to definitively resolve this issue [33].

During the 11-year solar cycle, significant changes occur in the structure of the heliospheric magnetic field. Our Sun emits a continuous radial stream of supersonic plasma, the so-called solar wind with an embedded solar magnetic field that develops into the HMF [31, 32]. Because the HMF remains rooted at the photosphere of the rotating Sun, it forms an Archimedean or so-called Parker spiral [32, 34, 35]. Over the years, many modifications to this field have been proposed, but the realization of Fisk (1996) [36] that the differential rotation of the Sun and the rigid rotation of polar coronal holes have a significant effect on the structure of the HMF led to second-generation global HMF models that are too complex [31]. The main attribute of the HMF is that it follows a 22-year cycle with a reversal approximately every  $\sim 11$  years at the time of extreme solar activity [31, 37]. When the  $\sim 11$ -year period is directed outward in the northern hemisphere and inward in the southern hemisphere, it is referred to as the  $A > 0$  solar magnetic cycle, and vice versa for the  $A < 0$  cycle (see figure 2 above).

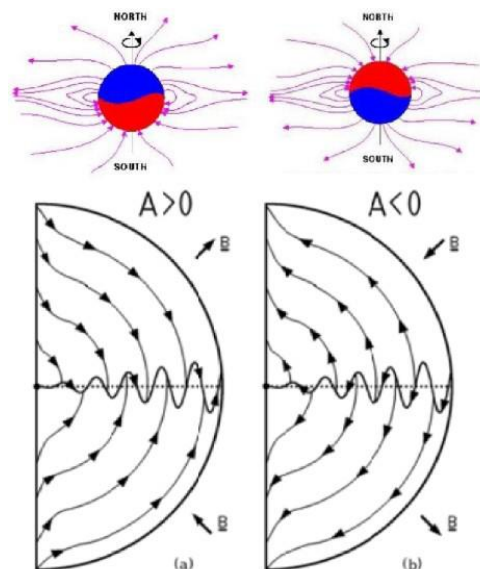


Figure 2. The idealistic picture of drift motion of positively charged particles at different polarities of the heliospheric magnetic field. During positive (left panel) /negative (right panel) polarity periods, the positively charged particles drift outward/inward along the heliospheric current sheet (Image from [31, 38]).

The largest structure of the HMF is the heliospheric current sheet (HCS). The HCS divides the heliosphere into regions with opposite polarities. The HCS demonstrates a wavy structure, parameterized by its tilt angle  $\alpha$  (this is the angle between the dipole axis of the solar magnetic field and the rotation axis of the Sun). The tilt angle  $\alpha$  determines the waviness of the HCS and correlates to solar activity. At high levels of solar activity,  $\alpha = 75^\circ$ , but then becomes undetermined during times of extreme solar activity, while during solar minimum  $\alpha = 3^\circ\text{--}10^\circ$  [31]. The waviness of the HCS has an important role in the CR modulation with the drift-dominated scenario, as discussed below.

The transport of cosmic rays in the heliosphere is formed by the combination of large-scale regular features and smaller-scale irregular fields [39]. The charged particles are scattered by irregularities in the heliospheric magnetic field, which is carried out with the solar wind. We describe the effects of this scattering as a diffusion process [40]. The magnetic field frozen into the solar wind tends to convect particles radially outward at the solar-wind speed. This sets up an outward gradient of cosmic rays that causes particles to diffuse inward [40, 41, 42]. In addition to the outward convection, the particles are subject to adiabatic cooling in the diverging solar wind [42]. The presence of a large-scale magnetic field affects the transport of particles. One effect of its presence is the existence of drifts [43]. Since there is a well-known difference in the cosmic ray modulation in successive polarity periods (see figure 3), it is important to consider particle drifts: gradient and curvature drifts as well as drift along the HCS [44]. Figure 2 shows idealistic global drift patterns for positively charged particles in  $A > 0$  and  $A < 0$  magnetic polarity cycles, together with a wavy HCS during solar minimum conditions [31].

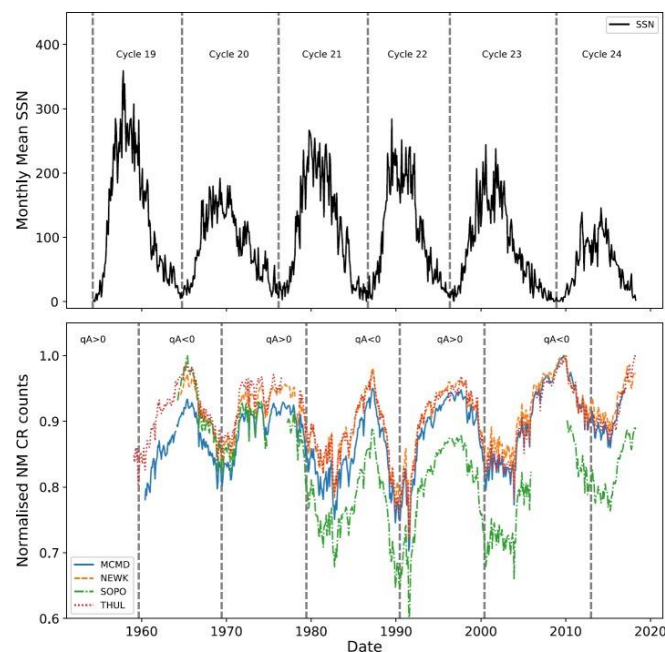


Figure 3. Monthly mean sunspot number (top), vertical lines indicate the beginning of each solar cycle. CR intensity recorded by NMs (bottom), vertical lines indicate the approximate epochs of solar magnetic-field polarity reversals (MCMD = McMurdo, NEWK = Newark, SOPO = South Pole, THUL = Thule) [45]. The time profiles of positively charged particles are more or less flat in the cycles with  $A > 0$  magnetic polarity like 1970s and 1990s, whereas in the cycles with  $A < 0$  magnetic polarity the time profiles are peaked like 1980s and 2000s (Image from [45]).

During the  $A > 0$  phase, when the field northward of the heliospheric current sheet (HCS) is directed outward, positively charged particles tend to drift towards the heliographic equator from the polar regions and drift outward along the HCS. When the polarity is reversed in the  $A < 0$  phase, positively charged particles drift inward along the current sheet, and outward via the polar regions of the heliosphere. Negatively charged particles (electrons, antiprotons, all antimatter nuclei) show the

opposite behavior. Therefore, the incoming GCR particles will be affected differently by the drift effects for the two magnetic configurations  $A > 0$  and  $A < 0$  [46]. As can be seen in figure 3, the 22-year solar magnetic cycle results in the alternating peaked and flat-topped shape of GCR intensity. The phenomenon is attributed to the “waviness” of the heliospheric current sheet (HCS) [47, 48]. Drifts may play an important role in cosmic ray transport during the period near solar minimum and 3–4 years after [39, 49]. However, it should be noted that perfect drift-dominated CR transport is not actually observed.

Although particle drifts are neglected in the simpler models of CR heliospheric modulation, more complex models explicitly take into account gradient, curvature and current sheet drifts in the HMF. Diffusion like propagation together with drifts, convection, and energy changes are the basic modulation mechanisms responsible for the 11- and 22-year variations in galactic cosmic ray intensity. Thus, the cumulative effects of the basic transport processes in the heliosphere are behind the solar modulation phenomenon of CRs [50]. The solar modulation is a space- and time-dependent phenomenon, i.e. it depends on where and when the CR flux is measured inside the heliosphere [50]. The spatial and temporal evolution of the GCR flux in the heliosphere can be described by the transport equation, introduced by Parker (1965) [51]. This equation is also known as the Parker transport equation.

### 5. Solutions of the cosmic ray transport equation

The Parker transport equation incorporates all modulation processes affecting the transport of GCRs inside the heliosphere [51]. In the heliocentric system, the Parker equation (also known as the cosmic ray transport equation) is expressed by [52]:

$$\frac{\partial U}{\partial t} = \frac{\partial}{\partial x_i} \left( K_{ij}^S \frac{\partial U}{\partial x_j} \right) - \frac{\partial}{\partial x_i} [(V_{sw,i} + v_{d,i})U] + \frac{1}{3} \frac{\partial V_{sw,i}}{\partial x_i} \frac{\partial}{\partial T} (\alpha_{rel} T U) \quad (5.1)$$

Here,  $U \equiv U(r, T, t)$  is the differential number density of particles with kinetic energy  $T$  at time  $t$  at a heliocentric radius  $r$ . The solar wind speed along the axis  $x_i$  is given by  $V_{sw,i}$ ,  $K_{ij}^S$  is the symmetric part of the diffusion tensor [51],  $v_d$  is the drift velocity,  $\alpha_{rel} = (T+2E_0)/(T+E_0)$  with  $E_0$  – the particle rest energy. For non-relativistic particles  $\alpha_{rel}(T) = 2$  and  $\alpha_{rel}(T) = 1$  for extremely relativistic particles [43] so that  $1 \leq \alpha_{rel} \leq 2$  [53].

The cosmic ray transport equation for stationary modulation in a spherically symmetric solar wind with constant speed  $V$ , under the assumption that the diffusion is isotropic [54, 55] has a form:

$$\frac{V}{r^2} \frac{\partial}{\partial r} (r^2 U_T) - \frac{1}{r^2} \frac{\partial}{\partial r} \left( r^2 k \frac{\partial U_T}{\partial r} \right) - \frac{2V}{3r} \frac{\partial}{\partial T} (\alpha_{rel} T U_T) = 0, \quad (5.2)$$

$U_T = U(r, T)$ ,  $[U_T] = \text{particles}/(\text{m}^3 \text{ T})$  [43]. The terms in equation (5.2) describe, from left to right, convection, diffusion of particles and energy loss in the expanding solar wind. The number density  $U$  is related to the differential intensity  $D$  as [51]:  $D = vU/4\pi$ ,  $v$  – the speed of the GCR particle.

The cosmic ray transport equation (TPE) is a partial differential equation of parabolic type [56]. In general, the equation cannot be solved analytically without simplifications. Due to its complexity, a numerical solution can be found when a realistic geometry of the heliosphere and a realistic functional form of the diffusion tensor are considered [57]. The first numerical solution of the TPE assuming a steady state and spherical symmetry was developed by Fisk (1971) [31, 55]. A brief history of the numerical models used to calculate cosmic ray intensities in the heliosphere can be found in [31, 58]. However, on the one hand, numerical modelling is a task that requires significant effort to accomplish [31]. On the other hand, the task concerning the GCR modulation has not been unambiguously solved theoretically because of insufficient knowledge of the properties of the modulation medium, the uncertainty of the boundary conditions (e.g., GCR energy spectra at the boundary of the modulation region), the time variations of these characteristics throughout the 11- and 22-year solar cycles [59, 60]. This motivates the use of simpler model solutions for practical purposes, such as the force-field and

diffusion-convection approximations. In [56], Moraal (2013) summarizes the hierarchy of the model approximations in increasing order of complexity.

In 1969, Lennard Fisk and William Ian Axford published approximate analytical solutions for the cosmic ray transport equation in the heliosphere [61]. One of their solutions is used to develop useful semi-empirical models (such as the Matthiä model [62], the Kuznetsov model [63], the Nymmik model [59, 64]) capable of predicting galactic spectra during the solar cycle [65].

## 6. Geomagnetic effects on galactic cosmic rays

After their modulation in the heliosphere, the CRs reach the Earth almost isotopically. The last hurdle that CRs have to overcome before entering the Earth's atmosphere is the magnetosphere. Particles with high rigidities are able to pass through the magnetosphere, so there are no long-lived trapped particles with high rigidities. For low-rigidity particles, Kallenrode (2004) [66] distinguishes three cases: a) particles hitting the low-latitude magnetosphere from the outside perform half a gyro-orbit inside the magnetosphere before being reflected back into space; b) these particles can only penetrate into the magnetosphere at the polar cusps and interacting with the atmosphere produce polar cap absorption (PCA) events; c) trapped particles forming long-lived radiation belts.

The Earth's magnetosphere is a vast comet-like region around the planet, dominated by the Earth's magnetic field. Galactic cosmic rays are charged particles and the Earth's magnetic field affects their trajectories. Depending on the altitude above Earth's surface, the magnetosphere provides varying degrees of protection from solar and galactic particles by attenuating particle fluxes with atmospheric depth [67]. While the low-energy particles of the solar wind are deflected around the magnetosphere and are cut off, cosmic rays with energies in the tens of MeV and greater have direct access to the inner magnetosphere [68].

The rigidity  $R$  is the most appropriate physical quantity describing the effect of magnetic field on charged particles. The  $R$  is connected to the Larmor radius  $r_L$  in a field of magnitude  $|\vec{B}|$  by

$$R = r_L |\vec{B}| c = cp/eZ \quad (6.1)$$

Because the energy (and  $pc$ ) is expressed in eV, the charge in terms of the number  $Z$  of elementary charges, i.e.  $Ze$ , where  $e = 1,602 \times 10^{-19}$  C, then  $R$  has units of Volts (V) [56]. CR particles with high rigidity (or energy) above a certain threshold will penetrate into the magnetosphere with nearly straight trajectories, while particles with intermediate rigidity will penetrate with a curved path, and the trajectories of low-rigidity particles will get strongly deflected such that they may even bounce back to their original direction of incidence [23]. This is the main reason why not all galactic particles that penetrate deep into the heliosphere reach the top of the Earth's atmosphere. Therefore, the intensity of galactic particles below certain energies, corresponding to the particle rigidity, is reduced [23]. It means that there is a screen effect for particles with a rigidity  $R$  below a threshold, called the cutoff rigidity  $R_c$  [69]. The charged particle cutoffs are a function of geomagnetic latitude, altitude, and the zenith and azimuthal directions and energy of the incident particle [67]. In the general case (except for geomagnetic cutoffs near the magnetic equator), the geomagnetic cutoff is "diffuse", i.e. at each position and in each direction there is an upper cutoff value  $R_U$  and a lower cutoff value  $R_L$  at the limits of an intermediate region, the so-called penumbral region [70]. Three regions can be distinguished.  $R_U$  is an upper cutoff value above which all particles have access to the point of interest. This is a region of high rigidities.  $R_L$  is a lower cutoff value below which particles cannot penetrate (forbidden regions). The region between the upper and lower cutoffs is an intermediate region, the so-called penumbra, where some cutoff values are allowed and others are not. Figure 4 illustrates trajectory-derived cutoff rigidities and the penumbral structure for the location at  $40^\circ$  latitude and  $0^\circ$  longitude.

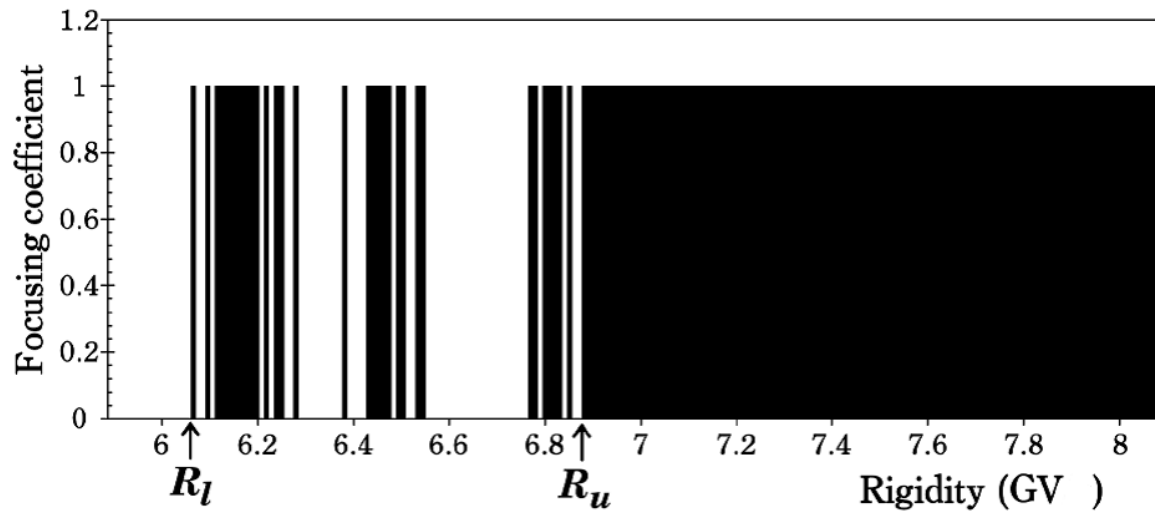


Figure 4. Illustration of the penumbra, i.e. the region of allowed and forbidden trajectories, calculated for the location: latitude =  $40^\circ$  and longitude =  $0^\circ$ . The direction of the trajectory is zenith =  $45^\circ$  and azimuth =  $0^\circ$ . The calculation is for a planetary radius of  $R_0 = 6448$  km, i.e. for the top of the Earth's atmosphere. White regions indicate forbidden rigidities, and black regions indicate allowed rigidities. Focusing and dispersion is not considered (Image from [71], adapted for this work).

As can be seen from figure 4, the geomagnetic cutoff is not sharp. There is the penumbra, in which allowed and forbidden trajectories alternate [71]. More about the geomagnetic effects on galactic cosmic rays can be found in [71, 72] and many others.

For computational reasons, however, the penumbra is often approximated by an effective cutoff ( $R_{\text{eff}}$ ) [71].  $R_{\text{eff}}$  lies between  $R_L$  and  $R_U$  and takes into account the transparency of the penumbra. In calculations, the effective cutoff rigidity is considered as a hard cutoff: all rigidities above  $R_{\text{eff}}$  are allowed and all rigidities below  $R_{\text{eff}}$  are forbidden [71]. At low latitudes, near the equator, the penumbra is covered almost by forbidden regions, i.e. it is almost completely “dark”, and at high latitudes, the penumbra is almost “transparent” [73]. The penumbra is most complex at middle latitudes: with many alternating bands of allowed and forbidden regions over a wide range of rigidity [73].

Since the calculation of a complete world grid of cutoff rigidities for a variety of directions takes a huge amount of time, the vertical cutoff approximation is the most widely used set of cutoff rigidities. The effective vertical cutoff rigidity,  $P_c$ , is a useful measure for comparing and interpreting particle measurements made at different locations on Earth, especially at different geomagnetic latitudes. The effective vertical cutoff rigidity  $P_c$  (often called vertical cutoff rigidity or simply cutoff rigidity) lies in the rigidity interval between the value below which (lower threshold) no particle arrives at the site of interest from the vertical direction and the highest rigidity value above which (upper threshold) all particles from that direction gain access.  $P_c$  depends strongly on the geomagnetic latitude, the altitude of the observation point, and the geomagnetic conditions at the time of observation [23]. The penumbral region is completely forbidden for vertical arrival between the equator and  $20^\circ$  geomagnetic latitude, but at higher latitudes alternate bands of allowed and forbidden rigidities are found and the penumbra becomes increasingly transparent [74].

The strength of the shielding effect of the geomagnetic field is greatest at the equator, where the field lines are parallel to the surface and the rigidity threshold is high. Here, all cosmic rays with energy less than  $\sim 15$  GeV cannot penetrate the upper atmosphere [6] and the number of incident particles is correspondingly low. However, the rigidity threshold decreases with increasing latitude and becomes weaker and weaker [6]. After the  $50^\text{th}$  parallel (or below the  $-50^\text{th}$  parallel), the cosmic ray intensity is no longer dependent on the latitude and becomes constant [6]. The cutoff rigidities for ground-based

cosmic ray stations and for vertical incidence are less than 1 GV near the magnetic poles and reach  $P_c \approx 15$  GV at the geomagnetic equator [75].

The computations of the propagation of cosmic ray particles in the Earth's magnetosphere are performed using computer programs based on numerical integration of the equation of motion [75]. The program package MAGNETOCOSMICS, kindly provided by Desorgher (2004) [76] from the University of Bern, can be used to calculate the effective vertical cutoff rigidity in a grid covering the whole Earth.

Kress *et al.* [68] point out that there is very little variation in cutoff rigidity with the direction of arrival for high-latitude cutoffs and this justifies the use of vertical cutoff rigidities for modelling the *omnidirectional cosmic ray flux* in low Earth orbit. However, vertical cutoff rigidities are not appropriate for modelling cosmic ray flux falling on geosynchronous or other equatorial orbits from all directions [68]. At low geomagnetic latitudes, low-energy cosmic rays from the east are suppressed compared to those from the west. The effect, known as the east-west effect, demonstrates that positively charged particles arriving from eastern directions exhibit much higher cutoff rigidities than particles with western directions of incidence. The strength of the effect increases with increasing zenith angle [77]. The east-west asymmetry is greatest near the geomagnetic equator and decreases towards higher latitudes [78]. Note that the effect is strongest at the top of the atmosphere and weakens at sea level due to collisions with atmospheric nuclei.

In more detailed studies, the transmission of particles through the cosmic ray penumbra must be considered more precisely. In this case, Smart *et al.* (2006) [70] define a penumbral transparency, a quantity that describes the particle flux transmitted through the penumbral region. When the penumbral transparency is about 1, it shows that most of the particle flux in the penumbral region is allowed through the geomagnetic field. Penumbral transparency approaching zero indicates that a very small part of the particle flux in the penumbral region is allowed through the geomagnetic field [70]. Here, we would like to point out that there is a fundamental property of the CR flux in the allowed range of rigidities. Assuming an isotropic CR flux in interplanetary space, Liouville's theorem demands that for rigidities above the cutoff rigidity, the directional flux of particles in the magnetosphere is equivalent to that outside the influence of the geomagnetic field [68, 79, 80, 81].

The properties of cosmic ray transport from the Earth's magnetosphere boundary at 1 AU to an observation point inside the magnetosphere can also be described by the so-called transmission function (TF) (see Bobik *et al.* (2006) [82]). Bobik *et al.* (2006) [82] determine the TF for different geomagnetic regions of AMS-01 orbit. In the penumbral region, where the particle rigidity is almost equal to the geomagnetic cutoff rigidity,  $0 < TF < 1$ .  $TF = 0$  in the forbidden region of rigidities, and  $TF = 1$  for rigidities above the cutoff rigidity.

The concepts of cutoff rigidities and asymptotic directions were developed to describe geomagnetic effects on primary GCRs. An asymptotic direction is the direction of motion of a cosmic particle before it enters the magnetosphere. The asymptotic directions need not be considered when the cosmic ray intensity varies isotropically in interplanetary space. But, when the cosmic ray intensity varies anisotropically, the asymptotic directions must be considered.

The solar modulated cosmic ray fluxes which we measure on the top of the Earth's atmosphere, are also known as the top of atmosphere (TOA) fluxes [21]. At most ground-based CR experiments, where mostly vertically incident particles contribute to the counting rate, it is assumed that only CRs with rigidities greater than the effective vertical cutoff rigidity  $P_c$  can reach the top of the Earth's atmosphere from all directions of incidence. However, at high altitudes and in sites with high cutoff rigidity or in space, the contribution of non-vertical incident particles becomes significant, and the variation of cutoff rigidity with the direction must be taken into account [83, 84, 85]. The database: <http://lpsc.in2p3.fr/crdb> provides easy and efficient access to cosmic ray data from various balloon and space experiments. These data contribute significantly to the understanding of the global aspects of the modulation and allow the development of more accurate empirical and semi-empirical models describing the cosmic ray spectra during the solar cycle. One such semi-empirical model is discussed in [86] on this issue.

Passing through the magnetic fields of the heliosphere and magnetosphere, GCRs strike the Earth's atmosphere. Primary CR particles with energies below several hundred MeV/nuc are simply stopped and absorbed in the atmosphere due to ionization losses [87]. However, if the energy of a primary particle is sufficiently high, it can interact with atmospheric nuclei and produce a cascade of secondary particles. In such collisions, many new particles are usually created and the colliding nuclei evaporate to a large extent [88]. During the development of the cascade (increase in the number of secondary particles), the flux of ionizing particles first increases down into the atmosphere, reaching its maximum [87] at altitude of 12–27 km (depending on season, solar activity level, and latitude), but then decreases with altitude due to the dominant absorption. Actually, on their way and in each interaction, the particles lose energy and eventually will not be able to generate new particles [88]. After some point, the shower maximum, more particles are stopped than generated, and therefore the number of shower particles decreases.

The altitude at which the flux of secondary particles is the largest is called the Pfozter maximum. The height of the Pfozter maximum varies with the geomagnetic latitude and solar cycle. Only a small fraction of the secondary particles usually comes down to the ground [88]. The number of secondary particles that actually reach the surface varies significantly depending on the energy and type of incident cosmic particles and the altitude (sea or mountain level). Atmospheric cascades initiated by higher-energy particles penetrate deeper into the atmosphere. However, for a given energy, heavier primary particles reach the shower maximum earlier, i.e. at shallower depths in the atmosphere than protons.

## 7. Conclusion

CR intensities and fluxes, as well as secondary particles that arrive on the ground, are of interest to scientists working in many different fields. It is believed that the beginning of the study of cosmic rays dates back to the pioneering balloon flights of Victor Hess, who measured the ionization of the atmosphere as a function of altitude. At the time, no one could have predicted that Victor Hess's flights would spawn new disciplines: astroparticle physics, high-energy astrophysics and elementary particle physics. Note that astroparticle physics is a relatively new field of research in which astrophysics, cosmology, cosmic rays, and particle physics work together to shed light on the nature and structure of matter in the universe [89]. It is often difficult to find a unique answer to the question "What is cosmic ray research?" This is because definitions can vary among the many professionals involved in cosmic ray research and because this field of research has encompassed many different areas of research throughout its long history [90]. In general, cosmic ray research involves the study of astrophysical systems, with scales ranging from the solar system, to our galaxy, to groupings of galaxies, focusing on the high energy processes that occur in these environments [90]. The galactic cosmic ray spectrum, at least for energies above  $10^2 - 10^3$  GeV/nuc, is fundamentally shaped by acceleration and diffusion; several other phenomena – e.g., convection, reacceleration, electromagnetic losses, and solar modulation – compete at lower energies [89]. The intensity of cosmic rays outside the Earth's magnetosphere depends on the local interstellar spectrum and its modulation in the heliosphere [91]. Note, however, that high-energy cosmic rays are not affected by the heliosphere.

Cosmic ray studies are not limited only to the traditional fields of high-energy physics and astronomy. Galactic cosmic rays are of interest to space weather researchers because they change radiation conditions in the near-Earth environment and can be considered an element of space weather. Furthermore, as dominant source of penetrating ionizing radiation, CRs affect physicochemical processes in the atmosphere. The energy input of CRs in the atmosphere is approximately equal to that of starlight and is about one-billionth of the solar irradiance [92]. However, cosmic ray ionization maintains the atmosphere as a very dilute electrically conducting plasma, allowing a continuous electrical current to pass from the ionosphere to Earth's surface [92]. The interaction of the CR particles with the atmosphere produces not only atmospheric ionization. The high-energy cosmic particles penetrating the dense layers of the atmosphere generate a rain of secondary cosmic rays, a small part of which continuously strikes the surface of the Earth. For example, about 20 primary particles arrive per square centimeter per second at the top of the atmosphere, while at sea level about one secondary cosmic

ray particle arrives per square centimeter per minute [93]. In order to calculate the energy and number of secondary particles together with their direction of arrival and the time variations of these variables, the fluxes and intensities of the particles arriving at the top of the Earth's atmosphere must be precisely determined; the influence of the geomagnetic field and the CR interaction with the Earth's atmosphere must also be taken into account. Among natural radiation sources, cosmic radiation contributes to about 10-15% of the total annual effective dose received by the population at ground level [94,95].

## References

- [1] *CERN Accelerating Science Cosmic Rays: Particles from Outer Space*  
Available from: <https://home.cern/science/physics/cosmic-rays-particles-outer-space>
- [2] *Cosmic Ray* Available from: [https://en.wikipedia.org/wiki/Cosmic\\_ray](https://en.wikipedia.org/wiki/Cosmic_ray)
- [3] Nelson G A 2016 *Radiat. Res.* **185** 349 Available from: <https://bioone.org/journals/radiation-research/volume-185/issue-4/RR14311.1/Space-Radiation-and-Human-Exposures-A-Primer/10.1667/RR14311.1.full>
- [4] Bazilevskaya G A 2000 *Space Sci. Rev.* **94**(1-2) 25
- [5] Butt Y 2009 *Nature* **460** 701
- [6] Ferrari F and Szuszkiewicz E 2009 *ASTROBIOLOGY* **9**(4) 413
- [7] Rand R J and Kulkarni S R 1989 *Astrophys. J.* **343** 760
- [8] Clay R W, Kurban Z and Wild N R 1998 *Cosmic Ray Related Undergraduate Experiments GAP Note 1998-061* Technical and Scientific Notes about the Pierre Auger Project (Pierre Auger Collaboration)
- [9] Gabici S, Evoli C, Gaggero D, Lipari P, Mertsch P, Orlando E, Strong A and Vittino A 2019 *Int. J. Mod. Phys. D*, **28** (15) 1930022
- [10] Siming Liu 2019 *Bulletin of the Chinese Academy of Sciences* **33**(3)
- [11] Tanabashi M et al. 2018 (and 2019 update) *Phys. Rev. D* **98** 030001
- [12] Mohrmann L et al. 2021 *PoS* **395** (37th Int. Cosmic Ray Conf. July 12th – 23rd, 2021 Berlin) 789
- [13] Abramowski A et al. 2016 *Nature* **531** 476
- [14] Kotera K and Olinto A V 2011 *Annu. Rev. Astron. Astrophys* **49** 119
- [15] Walz D S 2016 *Constraining Models of the Extragalactic Cosmic-Ray Origin with the Pierre Auger Observatory* Ph.D. Thesis (Aachen: RWTH Aachen University)
- [16] Ginzburg V I and Syrovatskii S I 1964 *The Origin of Cosmic Rays* (Oxford: Pergamon Press)
- [17] Wu J 2012 *Measurements of Cosmic Ray Antiprotons with PAMELA and Studies of Propagation Models* Doctoral Thesis (Stockholm: Royal Institute of Technology)
- [18] Schlaepfer H 2003 *Spatium* **11** (Association Pro ISSI) p 3 Available from: [http://www.issibern.ch/PDF-Files/Spatium\\_11.pdf](http://www.issibern.ch/PDF-Files/Spatium_11.pdf)
- [19] Ghia P L 2012 Cosmic ray detection *International School on AstroParticle Physics (Paris)*  
Available from:  
[https://isapp2012paris.sciencesconf.org/conference/isapp2012paris/P\\_Ghia\\_CosmicRayDetection\\_I.pdf](https://isapp2012paris.sciencesconf.org/conference/isapp2012paris/P_Ghia_CosmicRayDetection_I.pdf)
- [20] De Angelis A and Pimenta M 2018 *Introduction to Particle and Astroparticle Physics* (Cham: Springer)
- [21] Putze A 2006 *Propagation of Cosmic Rays in the Earth's Atmosphere* Thesis (Grenoble: Joseph Fourier University at Grenoble)
- [22] Longair M S 2011 *High Energy Astrophysics* (Cambridge: Cambridge University Press)
- [23] Mrigakshi A I 2013 *Galactic Cosmic Ray Exposure of Humans in Space* Dissertation (Kiel: Kiel University)
- [24] Esposito G 2002 *Study of Cosmic Ray Fluxes in Low Earth Orbit Observed with the AMS Experiment* PhD Thesis (Perugia: Università degli Studi di Perugia)
- [25] Pacini A A 2017 *Rev. Bras. Ens. Fis.* **39**(1) e1306
- [26] Bertaina M E 2014 *C R Phys* **15** 300
- [27] Dayananda M A 2013 *Correlation Studies of Cosmic Ray Flux and Atmospheric and Space*

- Weather* Dissertation (Atlanta: Georgia State University)
- [28] *Pierre Auger Observatory* Frequently Asked Questions  
Available from: <https://www.auger.org/outreach/cosmic-rays/faq>
- [29] Goldstein M L, Fisk L A and Ramaty R 1970 *Phys. Rev. Lett.* **25** 832
- [30] Mewaldt R A, Wiedenbeck M E, Scott L M, Binns W R, Cummings A C, Davis A .J, Israel M H, Leske R A, Stone E C and von Rosenvinge T T 2004 *AIP Conf. Proc.* **719** 127
- [31] Potgieter M S 2013 *Living Rev. Sol. Phys.* **10** 3
- [32] Gieseler J 2018 *Understanding Galactic Cosmic Ray Modulation: Observations and Theory* Dissertation zur Erlangung des Doktorgrades (Kiel: Faculty of Mathematics and Natural Sciences at Kiel University)
- [33] *The Sunspot Cycle* UCAR Center for Science Education Available from: <https://scied.ucar.edu/learning-zone/sun-space-weather/sunspot-cycle>
- [34] Owens M J and Forsyth R J 2013 *Living Rev. Sol. Phys.* **10** 5
- [35] Parker E N 1958 *Astrophys. J.* **128** 664
- [36] Fisk L A 1996 *J. Geophys. Res.* **101** 15547
- [37] Petrovay K and Christensen U R 2010 *Space Sci. Rev.* **155** 371
- [38] Laurenza M 2018 *14th Quadrennial Solar-Terrestrial Physics Symp.* 9-13 July Toronto
- [39] Jokipii J R and Kóta J 2000 *Astrophys. Space Sci.* **274** (1-2) 77
- [40] Fisk L A 1980 *Proc. Conf. Ancient Sun: Fossil Record in the Earth, Moon, and Meteorites* 16-19 October 1979 Boulder ed R. O. Pepin *et al.* (New York and Oxford: Pergamon Press) p 103
- [41] Perko J S 1984 *Solar Modulation of Galactic Cosmic Rays: Techniques & Applications* Ph.D. Thesis (Durham: University of New Hampshire)
- [42] Jokipii J R 1971 *Rev. Geophys.* **9**(1) 27
- [43] Batalha L 2012 *Solar Modulation Effects on Cosmic Rays* Dissertation (Lisbon: Instituto Superior Técnico)
- [44] Pei C, Bieber J W, Burger R A and Clem J 2012 *Astrophys. J.* **744**(2) 170
- [45] Ross E and Chaplin W J 2019 *Sol. Phys.* **294**(1) 8
- [46] Badruddin O P M Aslam 2012 *Sol. Phys.* **279** 269
- [47] Kóta J and Jokipii J R 1983 *Astrophys. J.* **265** 573
- [48] Zhao L-L, Qin G, Zhang M and Heber B 2014 *J. Geophys. Res.* **119**(3) 1493
- [49] McKibben R B, Connell J J, Lopate C, Simpson J A and Zhang M 1995 *Space Sci. Rev.* **72**(1-2) 367
- [50] Fiandrini E, Tomassetti N, Bertucci B, Donnini F, Graziani M, Khiali B and Reina Conde A 2021 *Phys. Rev. D* **104** 023012
- [51] Parker E N 1965 *Planet. Space Sci.* **13** 9
- [52] Bobik P *et al.* 2013 *AdAst* **2013** 793072
- [53] Gleeson L J 1968 *Proc. Astron. Soc. Aust.* **1**(4) (Clayton Victoria: Monash University) p 130
- [54] Cowsik R and Lee M A 1977 *Astrophys. J.* **216** 635
- [55] Fisk L A 1971 *J. Geophys. Res.* **76**(1) 221
- [56] Moraal H 2013 *Space Sci. Rev.* **176**(1-4) 299 Available from: <https://doi.org/10.1007/s11214-011-9819-3>
- [57] Zhang M 2008 *ASP Conf. Ser.* **385** 63
- [58] Manuel R 2013 *Time-dependent Modulation of Cosmic Rays in the Outer Heliosphere* Ph.D. Thesis (South Africa: North-West University)
- [59] Nymmik R A, Panasyuk M I, Pervaya T I and Suslov A A 1994 *Adv. Space Res.* **14**(10) 759
- [60] Nymmik R A and Suslov A A 1996 *Radiat. Meas.* **26**(3) 477
- [61] Fisk L A and Axford W I 1969 *J. Geophys. Res.* **74**(21) 4973
- [62] Matthiä D, Berger T, Mrigakshi A I and Reitz G 2013 *Adv. Space Res.* **51**(3) 329
- [63] Kuznetsov N V, Popova H and Panasyuk M I 2017 *J. Geophys. Res.* **122**(2) 1463
- [64] Nymmik R A, Panasyuk M I and Suslov A A 1996 *Adv. Space Res.* **17**(2) 19
- [65] Buchvarova M 2021 *Bulg. J. Phys.* **48**(1) 42

- [66] May-Britt Kallenrode 2004 *Space Physics: An Introduction to Plasmas and Particles in the Heliosphere and Magnetospheres* (Berlin Heidelberg: Springer-Verlag)
- [67] Barth J L 1997 Modeling space radiation environments *Notes from the 1997 IEEE NSREC Short Course* (Piscataway NJ: IEEE Publishing Services)
- [68] Kress B T, Hudson M K, Selesnick R S, Mertens C J and Engel M 2015 *J. Geophys. Res.* **120**(7) 5694
- [69] Fiandrini E *et al.* 2016 *PoS* **236** (34th Int. Cosmic Ray Conf. 30 July- 6 August 2015 The Hague The Netherlands) 095
- [70] Smart D F, Shea M A, Tylka A J and Boberg P R 2006 *Adv. Space Res.* **37**(6) 1206
- [71] Hirtz J and Leya I 2021 Dispersion and focusing of cosmic rays in magnetospheres arXiv:2104.13019
- [72] Vargas B and Valdés-Galicia J F 2011 *Proc. the 32th Int. Cosmic Ray Conf.* August 11-18 2011 Beijing China 1099
- [73] Biswas S 2000 *Cosmic Perspectives in Space Physics* Astrophysics and Space Science Library (Dordrecht: Kluwer Academic Publishers)
- [74] Quenby J J 1967 The time variations of the cosmic ray intensity *Kosmische Strahlung II / Cosmic Rays II* ed K Sitte *Handbuch der Physik/Encyclopedia of Physics* (Berlin Heidelberg: Newyork: Springer-Verlag) p 310
- [75] Bütikofer R. 2018 Cosmic ray particle transport in the Earth's magnetosphere *Solar Particle Radiation Storms Forecasting and Analysis* Astrophysics and Space Science Library ed O Malandraki and N Crosby (Cham: Springer) p 79
- [76] Desorgher L 2004 User guide of the MAGNETOCOSMICS code *Technical Report* (Bern: University of Bern)
- [77] Herbst K 2012 *Interaction of Cosmic Rays with the Earth's Magnetosphere and Atmosphere* Dissertation (Kiel: Kiel University)
- [78] Bhattacharya P C 1942 *Proc. R. Soc. London A* **8**(2) 263
- [79] Lemaitre G and Vallarta M S 1933 *Phys. Rev* **43**(2) 87
- [80] Swann W F 1933 *Phys. Rev* **44**(3) 224
- [81] Fermi E 1950 *Nuclear Physics* (Chicago IL: University of Chicago Press)
- [82] Bobik P, Boella G, Boschini M J, Gervasi M, Grandi D, Kudela K, Pensotti S and Rancoita P G 2006 *J. Geophys. Res.* **111** A05205
- [83] Clem J M, Bieber J W, Evenson P, Hall D, Humble J E and Duldig M 1997 *J. Geophys. Res.* **102** 26919
- [84] Dorman L I, Danilova O A, Iucci N, Parisi M, Ptitsyna N G, Tyasto M I and Villaresi G 2008 *Adv. Space Res.* **42** 510
- [85] Vainio R *et al.* 2009 *Space Sci. Rev.* **147** 187
- [86] Buchvarova M and Draganov D 2022 Model of galactic cosmic ray spectrum above the Earth's atmosphere *J. Phys.: Conf. Ser.* this issue
- [87] Mironova I A, Aplin K L, Arnold F, Bazilevskaya G A, Harrison R G, Krivolutsky A A, Nicoll, K A, Rozanov E V, Turunen E and Usoskin I 2015 *Space Sci. Rev.* **194** 1
- [88] *Cosmic-ray Air Showers*  
Available from: <https://www.mpi-hd.mpg.de/hfm/CosmicRay/Showers.html>
- [89] Castellina A and Donato F 2013 Astrophysics of galactic charged cosmic rays *Planets, Stars and Stellar Systems* ed T D Oswalt and G Gilmore (Dordrecht: Springer) 725
- [90] Wefel J P 1988 An overview of cosmic ray research: composition, acceleration and propagation *Genesis and Propagation of Cosmic Rays Nato ASI Series C: Mathematical and Physical Sciences* ed M M Shapiro and J P Wefel (Dordrecht: D. Reidel Publishing Company) 1
- [91] Fichtner H, Heber B, Herbst K, Kopp A and Scherer K 2013 Solar activity, the heliosphere, cosmic rays and their impact on the Earth's atmosphere *Climate and Weather of the Sun-Earth System (CAWSES)* ed F-J Lübken (Dordrecht: Springer) 55
- [92] Carlsaw K S, Harrison R G and Kirkby J 2002 *Science* **298**(5599) 1732

- [93] Close F, Marten M and Sutton C 2004 *The Particle Odyssey: A Journey to the Heart of Matter* (Oxford: Oxford University Press)
- [94] Radiation: Effects and Sources 2016 *United Nations Environment Programme* Available from: <http://large.stanford.edu/courses/2017/ph241/kwan2/docs/unep-2016.pdf>
- [95] Cinelli G *et al.* 2019 *European Atlas of Natural Radiation* ed G Cinelli *et al.* (Luxembourg: Publications Office of the European Union)